

Modeling of anomalous hysteresis behavior of compositionally graded ferroelectric films at low fields

C. K. Wong^{a)}

Department of Applied Physics, The Hong Kong Polytechnic University, Hong Kong, China

F. G. Shin

Department of Applied Physics, Materials Research Center and Center for Smart Materials, The Hong Kong Polytechnic University, Hong Kong, China

(Received 22 December 2004; accepted 29 May 2005; published online 20 July 2005)

We study the hysteresis behavior of compositionally graded ferroelectric films by theoretical simulations. Anomalous vertical (polarization) shift behavior of hysteresis loops measured by a Sawyer-Tower circuit at low/medium applied fields is investigated. The anomalous ferroelectric response is discussed by the use of a multilayer model to account for the variation of properties across the film thickness. Electrical conductivities of the ferroelectric layers have been taken into account and time-dependent space-charge-limited conduction has been adopted. The effects of charge mobility and the amplitude of applied field on the D - E loop shift were examined. Theoretical calculations are discussed in relation to the experimental data from previous works. © 2005 American Institute of Physics. [DOI: 10.1063/1.1985970]

I. INTRODUCTION

In the recent years, compositionally graded ferroelectric films have attracted great research interest for their unconventional ferroelectric properties that are not previously observed in nongraded ferroelectric films. Among these, the most notable phenomenon is the large polarization offset found in the hysteresis loop measurements when excited with a periodic alternating field.¹⁻⁴ Such properties may well lead to worthy device applications. Indeed, many workers have studied the ferroelectric properties of compositionally graded ferroelectric films experimentally,¹⁻⁷ and a few theoretical studies are also available in the literature. The works of Mantese *et al.*, Pintlilie *et al.*, and Ban *et al.* are examples which attempt to account for the polarization offset magnitudes, but not the dynamic response of the hysteresis loop.^{1,4,8} Chen *et al.* obtained an expression for the steady-state hysteresis loop and noted that the predicted offset did not fit their experimental data well.⁶ Recently, Poullain *et al.* suggested that asymmetrical leakage current could be responsible for the polarization offsets,⁹ and Bouregba *et al.* demonstrated this idea by setting diodes and resistors in parallel with a nongraded structure.¹⁰ They have not considered quantitative models for the asymmetrical leakage current and its interplay with the ferroelectric properties of the sample material. It seems that further theoretical input into the understanding and behavior of graded ferroelectrics, particularly as circuit components, is needed for future device applications.

In a previous paper, Chan *et al.* have suggested that time-dependent space-charge-limited conduction is a possible origin of the polarization offset and have demonstrated that the mechanism leads to asymmetric conduction and hence the polarization offsets.¹¹ The model can only be em-

ployed for high driving fields since their adopted P - E relation is not capable to model minor hysteresis loops (unsaturated loops). In this paper, the compositionally graded ferroelectric, placed in a Sawyer-Tower circuit, is modeled by a multilayer structure. The hysteresis model of Miller *et al.* is employed for each layer.^{12,13} This configuration is capable to describe both saturated and unsaturated loops of arbitrary fields. We will focus on low/medium applied fields which are rarely discussed previously. Assuming that electric, dielectric, and ferroelectric properties vary with composition across the film thickness, the polarization offset is then shown to strongly depend on the mobilities of charge carriers and the amplitude of the applied ac field. The offset follows a power-law dependence on the latter. The theoretical calculations are based on the experimental data for $\text{Pb}_{1-3y/2}\text{La}_y(\text{Zr}_{0.4}\text{Ti}_{0.6})\text{O}_3$ film [$x/40/60$ PLZT, $x(=100y)$ representing the La content]¹⁴ and for $\text{PbZr}_j\text{Ti}_{1-j}\text{O}_3$ film [PZT ($x, 1-x$), $x(=100j)$ representing the Zr content] with j varying from 0.55 to 0.75.

II. MULTILAYER MODEL FOR POLARIZATION-GRADED FERROELECTRICS

The Sawyer-Tower measurement circuit is merely a capacitor divider where the ferroelectric sample is in series with a standard reference capacitor. The electric displacement of the sample is calculated from the voltage measured across the standard capacitor. Usually two assumptions are made: electric displacements across the sample and standard capacitor are identical and the capacitance of the standard capacitor is much larger than that of the sample. This configuration for measuring the D - E loop of a compositionally graded ferroelectric film can be modeled by a multilayered structure with $n+1$ layers. The constitutive equation for the i th layer is

^{a)}Electronic mail: wongck.a@polyu.edu.hk

TABLE I. Properties of $\text{Pb}(\text{Zr}_{0.4}\text{Ti}_{0.6})\text{O}_3$ and 12/40/60 PLZT.

	$\varepsilon/\varepsilon_0^a$	σ_0 ($\Omega^{-1}\text{cm}^{-1}$)	μ_p ($\text{cm}^2/\text{V s}$)	μ_n ($\text{cm}^2/\text{V s}$)	P_r^a ($\mu\text{C}/\text{cm}^2$)	P_s^b ($\mu\text{C}/\text{cm}^2$)	E_c^b ($\text{V}/\mu\text{m}$)
PZT	420	10^{-12c}	2.5×10^{-12}	2.5×10^{-9}	11	20	8
PLZT	565	10^{-10}	2.5×10^{-12}	2.5×10^{-9}	19	40	8

^aReference 14.^bReference 4.^cReference 15.

$$D_i = P_i + \varepsilon_i E_i, \quad (1)$$

where D is the electric displacement, P is the polarization, ε is the permittivity, and E is the electric field, while i can be 1 to $n+1$. The first to n th layers represent in total the graded ferroelectric sample and the $(n+1)$ th layer represents the standard capacitor which is nonferroelectric [i.e., $P_{n+1}=0$ in Eq. (1)]. Moreover, the permittivity of the standard capacitor has been taken as 100 times the largest value among the permittivities of the graded ferroelectric layers.

When an external electric field E is applied in the thickness direction across the film,

$$E = \sum_{i=1}^{n+1} \nu_i E_i, \quad (2)$$

where $\nu_i = d_i / \sum_{j=1}^{n+1} d_j$ and d_i represents the i th layer thickness. In this work, we assume for convenience that the sample and standard capacitor have identical thickness, and that all ferroelectric layers of the sample have even thickness. We also assume that the sample material supports a finite conductivity so that charges may flow, thus the boundary conditions for two adjacent layers require

$$\begin{aligned} D_{k+1} - D_k &= q_k, \\ \sigma_k E_k - \sigma_{k+1} E_{k+1} &= \partial q_k / \partial t, \end{aligned} \quad (3)$$

where σ and q are the electrical conductivity and interfacial charge density, respectively. k can be 1 to n . The input impedance of the measuring oscilloscope can be modeled by setting a finite value for σ_{n+1} . Using Eqs. (1)–(3), we obtain

$$\begin{aligned} \alpha_k \frac{\partial E_{k+1}}{\partial t} + \beta_k E_{k+1} &= \sigma_k E + \varepsilon_k \frac{\partial E}{\partial t} - \nu_k \frac{\partial [P_{k+1} - P_k]}{\partial t} \\ &- \sum_{\substack{j=1 \\ j \neq k, k+1}}^{n+1} \nu_j \left[\sigma_k E_j + \varepsilon_k \frac{\partial E_j}{\partial t} \right], \end{aligned} \quad (4)$$

where $\alpha_k = \nu_k \varepsilon_{k+1} + \nu_{k+1} \varepsilon_k$ and $\beta_k = \nu_k \sigma_{k+1} + \nu_{k+1} \sigma_k$. Equation (4) constitutes n first-order differential equations. For a given external sinusoidal field E , we may obtain E_i as a function of time t when the P - E relations for the individual layers (P_i vs E_i) are known. Then the D - E loop of the “sample” (as measured by a Sawyer-Tower circuit) can be obtained from the electric field across the standard capacitor and the average electric field across the sample. In this work, the model of Miller *et al.* is used to describe the P - E relations of the constituent materials,^{12,13}

$$\frac{\partial P_i}{\partial E_i} = \left[1 - \tanh \sqrt{\frac{P_i - P_{\text{sat},i}}{\xi_i P_{s,i} - P_i}} \right] \frac{\partial P_{\text{sat},i}}{\partial E_i}, \quad (5)$$

where

$$P_{\text{sat},i} = \xi_i P_{s,i} \tanh \left[\frac{\xi_i E_i - E_{c,i}}{2E_{c,i}} \ln \left(\frac{1 + P_{r,i}/P_{s,i}}{1 - P_{r,i}/P_{s,i}} \right) \right]. \quad (6)$$

In this model, ξ_i takes +1 and -1 for increasing E_i and decreasing E_i , respectively. P_r , P_s , and E_c denote remanent polarization, saturation polarization, and coercive field, respectively. When solving Eq. (5) with Eq. (4), we use the relation $\partial P_i / \partial t = (\partial P_i / \partial E_i)(\partial E_i / \partial t)$.

It has been proposed that the polarization offset is an effect of the asymmetric leakage current. The time-dependent space-charge-limited current is a possible origin that gives rise to such an effect.¹¹ Electrical conductivity which varies temporally and spatially within the film is recently given by Chan *et al.* and is written as (see Appendix)

$$\begin{aligned} \sigma(x,t) &= \frac{\mu_p(x) - \mu_n(x)}{2} \frac{\partial D(x,t)}{\partial x} \\ &+ \sqrt{\left[\frac{\mu_p(x) + \mu_n(x)}{2} \frac{\partial D(x,t)}{\partial x} \right]^2 + \sigma_0(x)^2}, \end{aligned} \quad (7)$$

where $\mu_p(x)$ and $\mu_n(x)$ are the p -type and n -type mobilities, respectively, and σ_0 is the equilibrium conductivity. In solving Eqs. (4), (5), and (7), $\partial D(x,t) / \partial x$ in Eq. (7) may be written in a finite difference form to suit the multilayer structure.

III. COMPARISON WITH EXPERIMENTAL DATA

We will first concentrate on the calculation of the PLZT system of Boerasu *et al.*¹⁴ Their sample films were prepared by deposition of four PLZT layers with different La contents, followed by a rapid thermal annealing process. They measured the permittivity and remanent polarization of the four component materials, as well as the hysteresis loop of their 4/40/60 PLZT material. Both permittivity and remanent polarization were shown to increase with La content. Table I shows the constituent properties for $\text{Pb}(\text{Zr}_{0.4}\text{Ti}_{0.6})\text{O}_3$ and 12/40/60 PLZT used in our calculation; properties for PLZT with lesser La content were obtained by linear interpolation. As insufficient data on the constituent properties of $\text{Pb}(\text{Zr}_{0.4}\text{Ti}_{0.6})\text{O}_3$ and 12/40/60 PLZT were provided in their article, typical values based on other sources have been adopted in our calculation. Very few works have reported values for the electrical conductivity of PLZT. Jaffe *et al.* reported the conductivity for PZT as about $10^{-12} \Omega^{-1} \text{cm}^{-1}$,¹⁵

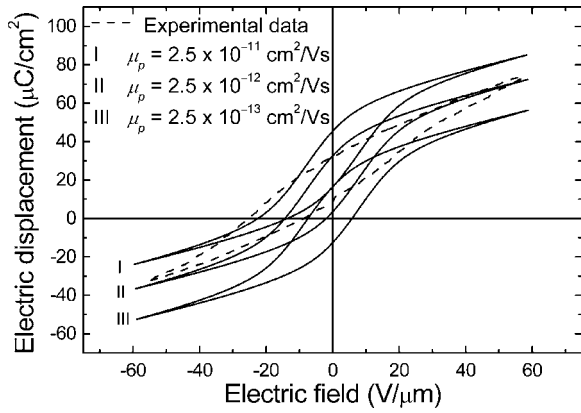


FIG. 1. Comparison of theoretical predictions for the D - E hysteresis loop of a PLZT-graded structure with the experimental data of Boerasu *et al.* (see Ref. 14).

while the measurement of Ray *et al.* gave a value of $4.6 \times 10^{-10} \Omega^{-1} \text{cm}^{-1}$ for $\text{Pb}_{0.9}\text{La}_{0.1}(\text{Zr}_{0.53}\text{Ti}_{0.47})_{0.975}\text{O}_3$.¹⁶ It seems that PLZT has larger conductivity than the PZT. We have therefore adopted $\sigma_0 = 10^{-12}$ and $10^{-10} \Omega^{-1} \text{cm}^{-1}$ for $\text{Pb}(\text{Zr}_{0.4}\text{Ti}_{0.6})\text{O}_3$ and 12/40/60 PLZT, respectively. Concerning the p -type and n -type mobilities, we follow Chan *et al.* to assume that μ_n is 1000 times μ_p .¹¹ A typical value for μ_p is about $2.5 \times 10^{-12} \text{cm}^2 \text{V}^{-1} \text{s}^{-1}$. We find that, although different μ_p values will not affect the direction of polarization offset, the magnitude of offset will be sensitive to the values of mobilities and we will demonstrate this in Fig. 1.

Figure 1 shows the D - E loop of the PLZT-graded structure measured at 50 Hz by Boerasu *et al.*,¹⁴ as well as the modeled results using 20 layers [i.e., $n=20$ in Eq. (4)] at the steady state (i.e., when no more increase in offset is observed) after the application of the external ac field. A high impedance oscilloscope is generally essential for a reliable measurement. Hence, σ_{n+1} has been set to a value which is equivalent to 100 G Ω of input resistance of the oscilloscope. The graded sample is modeled by using $\mu_n = 1000\mu_p$ with $\mu_p = 2.5 \times 10^{-11}$, 2.5×10^{-12} , and $2.5 \times 10^{-13} \text{cm}^2 \text{V}^{-1} \text{s}^{-1}$. The hysteresis loops are found to translate along the polarization axis as the simulation goes, reaching a stable offset value after some time. According to our simulation, these loops (shown in Fig. 1) should be very close to steady state after several minutes of measurement. However, a system with higher μ will generally take slightly more ac cycles to reach steady state. The modeled steady-state results reveal that the hysteresis loop will shift toward a larger offset value when μ increases. The measured result corresponds to a magnitude of polarization offset lying between the modeled results for $\mu_n = 2.5 \times 10^{-8}$ and $2.5 \times 10^{-9} \text{cm}^2 \text{V}^{-1} \text{s}^{-1}$ ("effective p -type mobility" between 2.5×10^{-11} and $2.5 \times 10^{-12} \text{cm}^2 \text{V}^{-1} \text{s}^{-1}$). Generally speaking, a high μ promotes the effect of polarization offset, but no offset can be produced in our calculation for a nongraded ferroelectric film (e.g., PZT) even if it possesses high μ . Concerning the direction of polarization offset, we find that it is determined by the direction of polarization gradient of the film. This is consistent with the experiments reported in the literature.¹⁻³

Figure 2 shows the modeled results with different applied field amplitudes when $\mu_n = 2.5 \times 10^{-9} \text{cm}^2 \text{V}^{-1} \text{s}^{-1}$. In

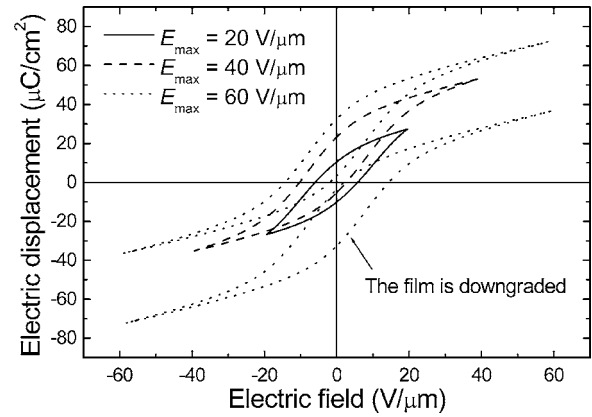


FIG. 2. Theoretical results of the D - E hysteresis loop of a PLZT-graded structure with different applied electric fields.

general, the magnitude of polarization offset increases as the amplitude of applied field increases. On the other hand, the width of the loops also increases as the field amplitude increases and this feature is always observed in the past experiments.^{3,6,17} However, this phenomenon did not emerge from the results of the model of Chan *et al.* which was not quite suitable for modeling minor hysteresis loops. When the amplitude of applied field is limited, many layers in the sample trace minor hysteresis loops (unsaturated loops) and the width of the resultant loop is also small. The modeled result for a downgraded film is also shown in Fig. 2. This is obtained by reversing the gradient of all constituent properties.

For an upgraded film employing $E_{\text{max}} = 60 \text{V}/\mu\text{m}$, the dynamic profile of the polarization shift magnitude is illustrated in Fig. 3, which is similar to the charging of a capacitor. This agrees with the experimental results of Brazier *et al.*⁵ They also suggested that this time-dependent behavior was controlled by the RC behavior of the Sawyer-Tower components and an expression had been proposed. In our previous work, we have derived explicit expressions for the dynamic behavior of a ferroelectric film with symmetric (Ohmic) conductivity and for the saturated remanent polarization values of a ferroelectric film with asymmetric conductivity. The time taken to reach steady state has been found to also depend on the electric, dielectric, and ferroelec-

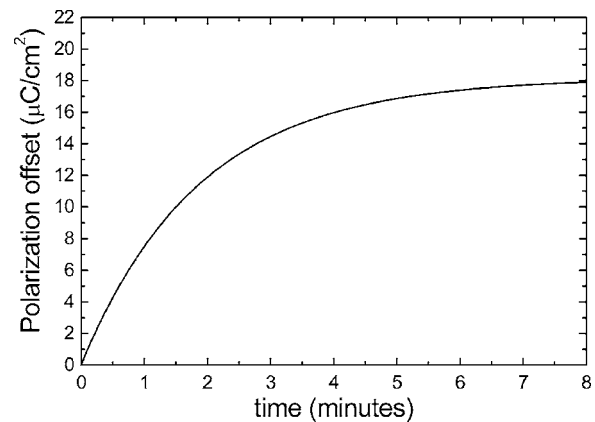


FIG. 3. The time development of the polarization offset of a PLZT-graded structure with $E_{\text{max}} = 60 \text{V}/\mu\text{m}$ and $\mu_n = 2.5 \times 10^{-9} \text{cm}^2 \text{V}^{-1} \text{s}^{-1}$.

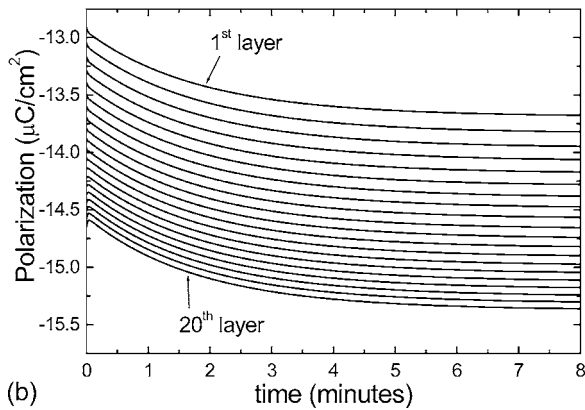
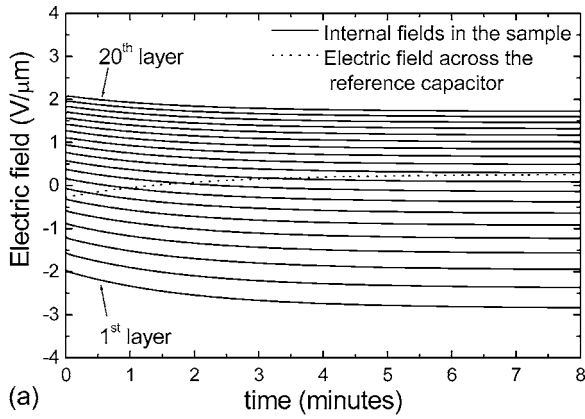


FIG. 4. The time development of the (a) electric field and (b) polarization in the constituents of a PLZT-graded structure with $E_{\max}=60 \text{ V}/\mu\text{m}$ and $\mu_n=2.5 \times 10^{-9} \text{ cm}^2 \text{ V}^{-1} \text{ s}^{-1}$.

tric properties of the sample, as well as the frequency of the applied field in a complicated manner.¹⁸ Our simulation for graded ferroelectrics also reveals that the properties of the layers strongly affect this dynamics. It is found that more ac periods are required for reaching the steady state, when the sample conductivity is decreased in the calculation. On the other hand, a higher frequency also means more cycles to reach the steady state, but not necessarily requiring a longer duration of measurement. However, analytical expressions to characterize the dynamic behavior for graded ferroelectrics are difficult to obtain.

Figures 4(a) and 4(b) show the dynamics of the values of electric field after each ac period and the polarization distribution of a graded film with 20 layers, i.e., only the electric field and polarization when t is a multiple of 0.2 s are shown. The adopted constituent properties are identical to the set in Fig. 3. In Fig. 4(a), the electric field spreads out over a wide range of values with a minimum at the first layer and maximum at the 20th layer. In other words, there is a large spread in electric field across the film thickness and this spread progressively increases until saturation (see Fig. 5). If a graded ferroelectric sample possesses zero conductivity, there will be no progressive increment of spread in the electric field. An important note from Fig. 4(a) is, since the field values in the sample decrease progressively, the electric field across the reference capacitor thus progressively increases. In Fig. 4(b), information about the time-dependent polarization gra-

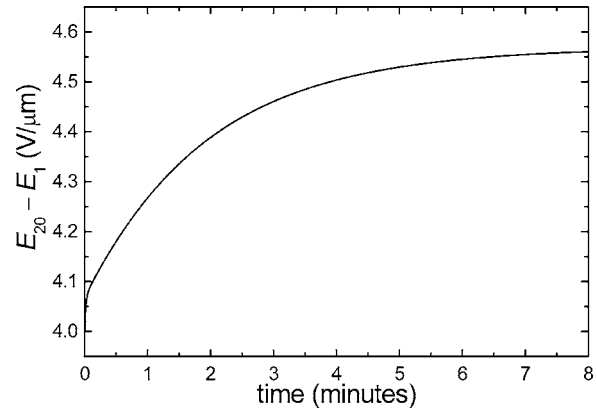


FIG. 5. The progressive increment of the spread in electric field between the first and 20th layers of a PLZT-graded structure with $E_{\max}=60 \text{ V}/\mu\text{m}$ and $\mu_n=2.5 \times 10^{-9} \text{ cm}^2 \text{ V}^{-1} \text{ s}^{-1}$.

dent within the sample is shown. Since we have set the P_r 's to monotonically increase from the first layer to the 20th layer, the polarization has the largest magnitude at the 20th layer and the smallest magnitude at the first layer.

In Fig. 6, the time-dependent conductivity for the first 5 s is shown. The distribution of conductivity $\sigma(t)$ across the film thickness is very close to the distribution of σ_0 which varies from 10^{-12} to $10^{-10} \text{ } \Omega^{-1} \text{ cm}^{-1}$. Apart from the first half second, the change of conductivity $\sigma(t)$ after each period is small.

Now we come to a $\text{PbZr}_j\text{Ti}_{1-j}\text{O}_3$ system with j varying from 0.55 to 0.75; our adopted properties for PZT (55,45) and PZT (75,25) are shown in Table II. Similar to the treatment of the previous PLZT system, the properties for other compositions of PZT were obtained by linear interpolation. Moreover, we assume that P_s is 10% larger than P_r . The electrical conductivity of a PZT can vary quite sensitively with the impurity level and device structure.^{19,20} For the illustration of the effect of high conductivity in some situations, we assume that the film possesses high-conductivity values. For low-conductivity films, it generally takes more ac cycles in the simulations to reach steady state unless the input impedance of the measuring oscilloscope has a lower value such as that demonstrated by Chan *et al.*¹¹ In addition, the conductivity for PZT (55,45) is assumed to be smaller

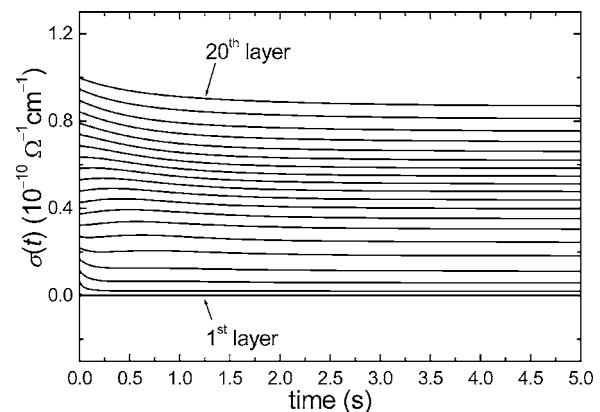


FIG. 6. The first 5 s of the time-dependent conductivity in the constituents of a PLZT-graded structure with $E_{\max}=60 \text{ V}/\mu\text{m}$ and $\mu_n=2.5 \times 10^{-9} \text{ cm}^2 \text{ V}^{-1} \text{ s}^{-1}$.

TABLE II. Properties of PZT (55/45) and PZT (75/25). Symbol j represents the composition of Zr in $\text{PbZr}_j\text{Ti}_{1-j}\text{O}_3$.

j	ϵ/ϵ_0^a	σ_0 ($\Omega^{-1}\text{cm}^{-1}$)	μ_p^b ($\text{cm}^2/\text{V s}$)	μ_n^b ($\text{cm}^2/\text{V s}$)	P_r^a ($\mu\text{C}/\text{cm}^2$)	P_s ($\mu\text{C}/\text{cm}^2$)	E_c^a ($\text{V}/\mu\text{m}$)
0.55	580	1.33×10^{-10}	2.5×10^{-9}	2.5×10^{-6}	33	36.3	4.3
0.75	450	2.5×10^{-10}	2.5×10^{-9}	2.5×10^{-6}	36	39.6	2.5

^aReference 21.^bReference 11.

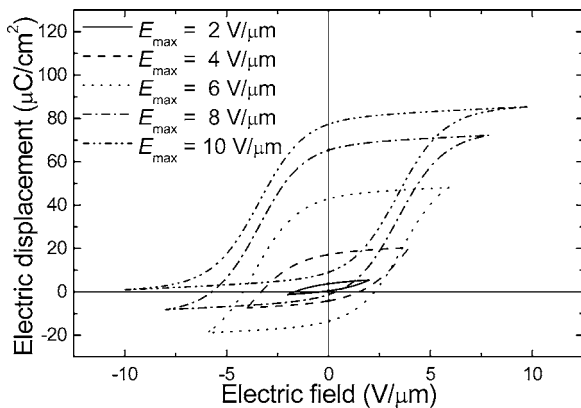
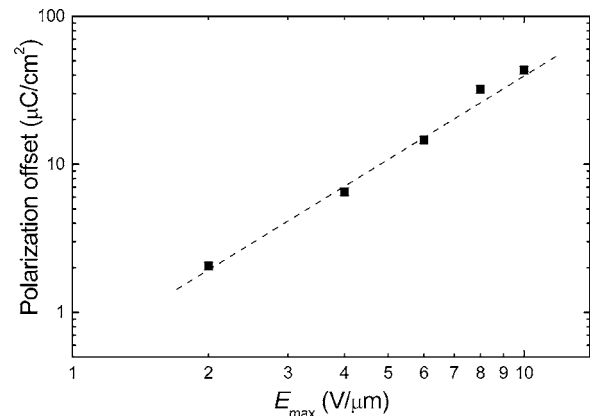
than that for PZT (75,25).²¹ The modeled results at steady state for five different applied field amplitudes are shown in Fig. 7. The frequency of the applied field was taken as 100 Hz and $n=20$ in the calculation. The phenomenon that the magnitude of polarization offset increases for increasing field amplitudes is evident and approximately obeys a power law. Figure 8 shows that the polarization offset is proportional to $E_{\text{max}}^{1.96}$.

In a previous work, Brazier *et al.* measured the polarization offset (P_{off}) of $\text{PbZr}_j\text{Ti}_{1-j}\text{O}_3$ with j varying from 0.55 to 0.75.² They found a power-law dependence of $P_{\text{off}} \sim E_{\text{max}}^\gamma$ with $\gamma=5$ at large applied fields. However, their experimental data reveal another power-law dependence of $P_{\text{off}} \sim E_{\text{max}}^{1.6}$ when E_{max} is smaller than the coercive field of PZT. In another report, their measured values also revealed a $\gamma \approx 1.79$ for the same composition of a graded PZT film within the low-field regime ($E_{\text{max}} \leq 10 \text{ V}/\mu\text{m}$), and the value of γ is also larger within the regime of high driving fields.²² In Figs. 7 and 8, we focus on the effect of small to medium applied field. We obtain a power-law dependence of $P_{\text{off}} \sim E_{\text{max}}^{1.96}$ for E_{max} varying from 2 to 10 $\text{V}/\mu\text{m}$. This finding suggests that the space-charge-limited current is able to describe the power-law relationship of graded ferroelectrics at the small to medium field region such as that demonstrated by Brazier *et al.* If high driving fields are adopted in the simulation and all layers in the sample trace saturated loops, larger value of γ will be obtained (>3) such as that demonstrated by Chan *et al.*¹¹ In reality, many measurements on the polarization offset of graded ferroelectrics reported some larger γ at high applied fields ($\gamma \approx 2-5$) and the same compositionally graded film can also give vastly different γ 's for upgraded and downgraded films.^{3,17,23-25} This suggests that other conduction mechanisms may become significant at the high-field

regimes. A more rigorous calculation applicable from low to high fields may need to include other conduction mechanisms as well as the substrate effect and/or the film-electrode interaction. Nevertheless, the phenomenon that larger field amplitude leads to larger polarization offset remains the same from low to high applied fields.

IV. CONCLUSIONS

In conclusion, simulations of the anomalous polarization offset in compositionally graded ferroelectric films have been performed. The variations of the constituent parameters are implemented by the use of a multilayer model, and the conduction behavior is described by a time-dependent space-charge-limited current. Both a higher mobility of charge carriers and larger amplitude of applied field will enhance the effect of polarization offset, as have been illustrated using the experimental values of the PLZT system of Boerasu *et al.*¹⁴ as well as a PZT system with Zr content varying from 0.55 to 0.75. Our results reveal that a characteristic feature associated with the dynamic polarization offset phenomenon is the progressively increasing spread in the internal field across the film thickness preferentially toward lower-field values (or alternatively toward higher-field values). The resulting P_{off} vs E_{max} relationship seems to indicate that the present model is appropriate for discussing the offset phenomena in the regime of small to medium field magnitudes, when the ferroelectric layers (or some of them) trace minor hysteresis loops.

FIG. 7. Theoretical results of the D - E hysteresis loop of a PZT-graded structure with different applied electric fields.FIG. 8. The variation of polarization offset with the magnitude of electric field across sample. The polarization offset is approximately proportional to $E_{\text{max}}^{1.96}$.

ACKNOWLEDGMENT

This work was partially supported by the Center for Smart Materials of The Hong Kong Polytechnic University.

APPENDIX: TIME-DEPENDENT SPACE-CHARGE-LIMITED CONDUCTION

Assuming that a ferroelectric sample consists of p -type and n -type free charge carriers and their mobilities are denoted by $\mu_p(x)$ and $\mu_n(x)$, respectively, where both can generally be functions of position x , then the time-dependent electrical conductivity can be written as

$$\sigma(x,t) = \sigma_0(x) + e\{\mu_p(x)\Delta p(x,t) + \mu_n(x)\Delta n(x,t)\}, \quad (\text{A1})$$

where

$$\sigma_0(x) = e\{\mu_p(x)p_i(x) + \mu_n(x)n_i(x)\} \quad (\text{A2})$$

and symbols e and σ_0 represent the magnitude of electronic charge and the conductivity in equilibrium, respectively. $\Delta p(x,t)$ and $\Delta n(x,t)$ denote the change of charge concentrations at time t . The intrinsic charge concentrations $p_i(x)$ [for p -type carrier] and $n_i(x)$ [for n -type carrier] are identical (due to charge neutrality). The law of mass action gives

$$p_i(x) = n_i(x) = \sqrt{[p_i(x) + \Delta p(x,t)][n_i(x) + \Delta n(x,t)]}. \quad (\text{A3})$$

Using Gauss's law for electric displacement,

$$\frac{\partial D(x,t)}{\partial x} = e[p_i(x) + \Delta p(x,t)] - e[n_i(x) + \Delta n(x,t)]. \quad (\text{A4})$$

We may solve the system of quadratic equations [Eqs. (A3) and (A4)] to obtain $\Delta p(x,t)$ and $\Delta n(x,t)$. Making use of Eq. (A2), we then substitute $p_i(x) = n_i(x) = \sigma_0(x)/e/[\mu_p(x) + \mu_n(x)]$. The results are

$$\begin{aligned} \Delta p(x,t) &= \frac{1}{2e} \left[\pm \sqrt{\left(\frac{\partial D(x,t)}{\partial x}\right)^2 + \frac{4\sigma_0(x)^2}{[\mu_p(x) + \mu_n(x)]^2}} \right. \\ &\quad \left. + \frac{\partial D(x,t)}{\partial x} - \frac{2\sigma_0(x)}{\mu_p(x) + \mu_n(x)} \right], \\ \Delta n(x,t) &= \frac{1}{2e} \left[\pm \sqrt{\left(\frac{\partial D(x,t)}{\partial x}\right)^2 + \frac{4\sigma_0(x)^2}{[\mu_p(x) + \mu_n(x)]^2}} \right. \\ &\quad \left. - \frac{\partial D(x,t)}{\partial x} - \frac{2\sigma_0(x)}{\mu_p(x) + \mu_n(x)} \right]. \end{aligned} \quad (\text{A5})$$

The solution is only valid for the positive square root. Thus, Eq. (A1) becomes

$$\begin{aligned} \sigma(x,t) &= \frac{\mu_p(x) - \mu_n(x)}{2} \frac{\partial D(x,t)}{\partial x} \\ &\quad + \sqrt{\left[\frac{\mu_p(x) + \mu_n(x)}{2} \frac{\partial D(x,t)}{\partial x}\right]^2 + \sigma_0(x)^2}. \end{aligned} \quad (\text{A6})$$

- ¹J. V. Mantese, N. W. Schubring, A. L. Micheli, A. B. Catalan, M. S. Mohammed, R. Naik, and G. W. Auner, *Appl. Phys. Lett.* **71**, 2047 (1997).
- ²M. Brazier, M. McElfresh, and S. Mansour, *Appl. Phys. Lett.* **72**, 1121 (1998).
- ³D. Bao, X. Yao, and L. Zhang, *Appl. Phys. Lett.* **76**, 2779 (2000).
- ⁴L. Pintilie, I. Boerasu, and M. J. M. Gomes, *J. Appl. Phys.* **93**, 9961 (2003).
- ⁵M. Brazier, M. McElfresh, and S. Mansour, *Appl. Phys. Lett.* **74**, 299 (1999).
- ⁶Z. Chen, K. Arita, M. Lim, and C. A. Paz De Araujo, *Integr. Ferroelectr.* **24**, 181 (1999).
- ⁷G. Jamn, K.-S. Liu and I.-N. Lin, *Integr. Ferroelectr.* **31**, 77 (2000).
- ⁸Z.-G. Ban, S. P. Alpay, and J. V. Mantese, *Phys. Rev. B* **67**, 184104 (2003).
- ⁹G. Poullain, R. Bouregba, B. Vilquin, G. Le Rhun, and H. Murray, *Appl. Phys. Lett.* **81**, 5015 (2002).
- ¹⁰R. Bouregba, G. Poullain, B. Vilquin, and G. Le Rhun, *J. Appl. Phys.* **93**, 5583 (2003).
- ¹¹H. K. Chan, C. H. Lam, and F. G. Shin, *J. Appl. Phys.* **95**, 2665 (2004).
- ¹²S. L. Miller, R. D. Nasby, J. R. Schwank, M. S. Rodgers, and P. V. Dressendorfer, *J. Appl. Phys.* **68**, 6463 (1990).
- ¹³S. L. Miller, J. R. Schwank, R. D. Nasby, and M. S. Rodgers, *J. Appl. Phys.* **70**, 2849 (1991).
- ¹⁴I. Boerasu, L. Pintilie, and M. Kosec, *Appl. Phys. Lett.* **77**, 2231 (2000).
- ¹⁵B. Jaffe, W. R. Cook, Jr., and H. Jaffe, *Piezoelectric Ceramics* (Academic, London, 1971).
- ¹⁶J. Ray, P. Hing, and R. N. P. Choudhary, *Mater. Lett.* **51**, 434 (2001).
- ¹⁷D. Bao, N. Mizutani, X. Yao, and L. Zhang, *J. Appl. Phys.* **89**, 801 (2001).
- ¹⁸C. K. Wong, C. H. Tsang, and F. G. Shin, *J. Appl. Phys.* **96**, 575 (2004).
- ¹⁹J. J. Dih and R. M. Fulrath, *J. Am. Ceram. Soc.* **61**, 448 (1978).
- ²⁰H. S. Nalwa, *Handbook of Thin Film Materials* (Academic, San Diego, 2002), Vol. 3, p. 61.
- ²¹C. M. Foster, G.-R. Bai, R. Csencsits, J. Vetrone, R. Jammy, L. A. Wills, E. Carr, and J. Amano, *J. Appl. Phys.* **81**, 2349 (1997).
- ²²M. Brazier, S. Mansour, and M. McElfresh, *Ferroelectric Thin Films VII Symposium*, MRS Symposia Proceedings (Materials Research Society, Warrendale, 1999), 541, p. 507.
- ²³D. Bao, N. Mizutani, X. Yao, and L. Zhang, *Appl. Phys. Lett.* **77**, 1041 (2000).
- ²⁴D. Bao, N. Mizutani, X. Yao, and L. Zhang, *Appl. Phys. Lett.* **77**, 1203 (2000).
- ²⁵D. Bao, N. Wakiya, K. Shinozaki, N. Mizutani, and X. Yao, *J. Appl. Phys.* **90**, 506 (2001).